Journal of Asian Earth Sciences 163 (2018) 22–31

Contents lists available at ScienceDirect

Journal of Asian Earth Sciences

journal homepage: www.elsevier.com/locate/jseaes

Full length article

Present-day crustal deformation characteristics of the southeastern Tibetan Plateau and surrounding areas by using GPS analysis

Wei Qu[a,b], Zhong Lu[b,*], Qin Zhang[a], Ming Hao[c], Qingliang Wang[c], Feifei Qu[b], Wu Zhu[a]

[a] College of Geology Engineering and Geomatics, Chang' an University, Xian, Shaanxi, China
[b] Department of Earth Sciences, Southern Methodist University, Dallas, TX, USA
[c] Second Monitoring and Application Center, CEA, Xian, Shaanxi, China

ARTICLE INFO

Keywords:
Crustal deformation
Strain field
Southeastern Tibetan Plateau
GPS
Geodynamics

ABSTRACT

The southeastern Tibetan Plateau and surrounding areas comprise a typical tectonic belt in mainland China, characterized by a complex geological background and intense tectonic activity. We study present-day crustal deformation characteristics of this region based on GPS data for the periods 1999–2007 and 2009–2011. We first analyze the variations in crustal motion and strain rate, and then discuss the 3D crustal motion and local sub-block activities, as well as the correlation between the intensity of crustal activity and the strain rate distribution. Finally, we explain the present-day geodynamic characteristics of the region. Our results indicate that the entire region shows overall clockwise motion with respect to the stable Eurasian Plate. The tectonic boundary belts between this region and the South China Block display significant compressional strain, accompanied by associated extensional strain. Relatively high maximum shear strain and the transition zones of the significant plane strain gradients are also mainly concentrated along the Ganzi–Yushu–Xianshuihe, Anninghe–Zemuhe–Xiaojiang, Lijiang–Xiaojinhe, and Red River faults, as well as the western and southern Yunnan Province. 3D crustal velocities further reflect significant differences in tectonic activity between different structural belts. We conclude that the regions showing higher shear strain and the transition zones of the significant plane strain gradients correspond to the areas with frequent earthquakes. According to the crustal deformation and strain characteristics, we infer that the present-day geodynamic setting of the region is related to the ongoing India–Eurasia collision and the associated resistance of the stable Alashan, Ordos, and South China blocks, resulting in the extrusion of the southeastern Tibetan Plateau crustal material with an overall clockwise flow around the Eastern Himalayas and significant compressional strain along the tectonic boundary belts. Furthermore, notable compressional strain and enhanced sub-block motions occurred around the Longmenshan fault area following the Wenchuan earthquake.

1. Introduction

The southeastern Tibetan Plateau (SETP) is an important passageway for the materials of the Tibetan Plateau moving toward the southeast, and as a result, this region comprises an intense tectonic belt in mainland China (Fig. 1, Chen et al., 2013a; Royden et al., 2008; Zhu et al., 2017; Li et al., 2016a; Wang et al., 2017). In recent years, many studies have revealed various important characteristics of the SETP and surrounding areas. The continental dynamic setting and stress evolution was simulated using numerical simulation models (Liu et al., 2007; Yang and Liu, 2009; Bai et al., 2010; He et al., 2011; White and Lister, 2012; Chen et al., 2013b; Liu et al., 2015; Liu et al., 2016). The tectonics of faults and earthquakes were described by field investigations and focal mechanism data (Lin et al., 2014; Shi et al., 2016; Zhang and Wang, 2007; Shao et al., 2016; Fu et al., 2011; Lin et al., 2011). The velocities of the active faults were investigated using GPS, InSAR and leveling observations (Chen et al., 2015; Jiang et al., 2014; Shen et al., 2009; Zou et al., 2015; Liu et al., 2011; Wang et al., 2011; Gan et al., 2007; Liang et al., 2013; Wu et al., 2015a; Xu and Stamps, 2016; Zhang et al., 2013a,b; Chang et al., 2017; Hao et al., 2014). The deep structure of the crust was also explored by seismic wave velocity and Bouguer gravity data (Robert et al., 2010; Jiang et al., 2012; Chen et al., 2013a; Cai et al., 2016; Li et al., 2016b).

These aspects of the continental dynamic setting, fault slip rates, seismic activities, stress evolution, deep structures, and crustal activities are of great importance for better understanding of the geodynamics of the SETP. Among the above-mentioned methods, GPS technology has great advantages in providing crustal motion data with

* Corresponding author.
E-mail address: zhonglu@smu.edu (Z. Lu).

https://doi.org/10.1016/j.jseaes.2018.05.021
Received 6 January 2018; Received in revised form 31 March 2018; Accepted 25 May 2018
Available online 26 May 2018
1367-9120/

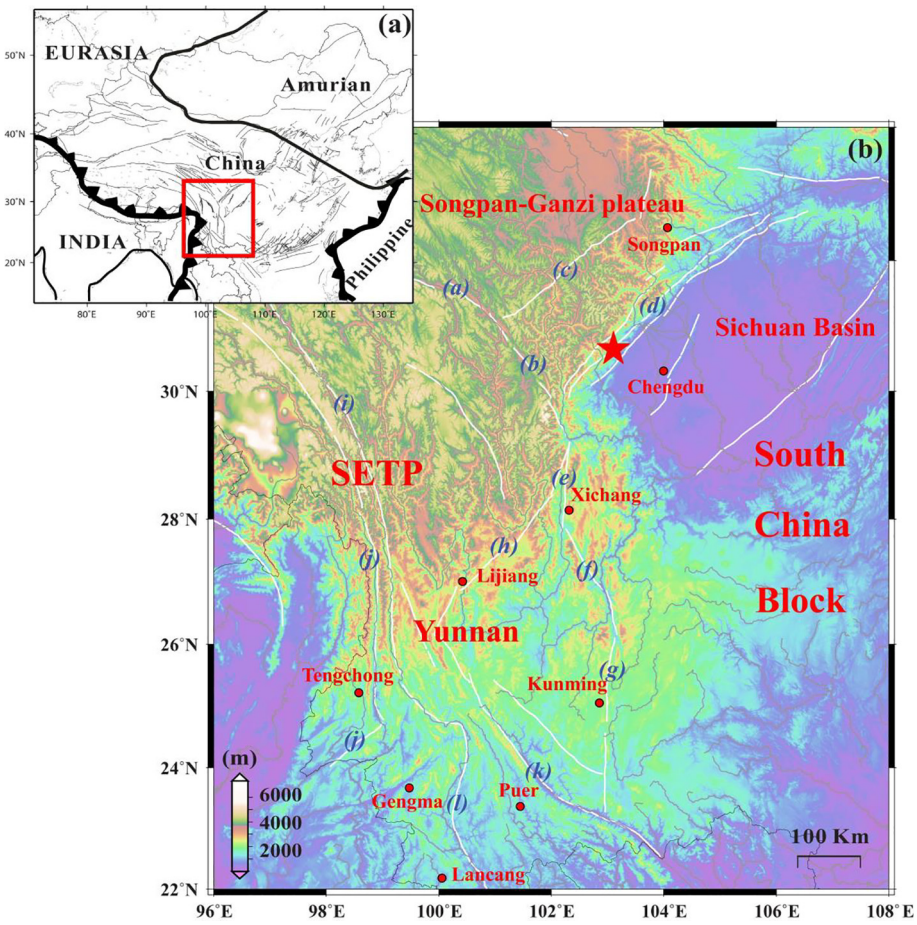

Fig. 1. Location of the SETP and its surroundings in China, as well as the major plate boundaries in and near mainland China (Fig. 1a). The red dashed box indicates the SETP and its adjacent tectonic belts (Fig. 1b). The white solid lines represent the major active faults (Zhang et al., 2005). The small red circles represent major cities. The red star indicates the epicenter of the Wenchuan earthquakes. The italic alphabet characters represent the major faults of the SETP, such as Ganzi-Yushu (a), Xianshuihe (b), Longriba (c), Longmenshan (d), Anninghe (e), Zemuhe (f), Xiaojinghe (g), Lijiang–Xiaojinhe (h), Jinshajiang (i), Nujiang (j), Red River (k), Lancangjiang (l).

higher spatial resolution and more flexible timescales, and can also effectively reflect the present-day dynamic processes. However, although GPS data have been used to describe the general characteristics of crustal activity of the SETP within a certain time period, the detailed variations in crustal deformation and strain fields before and after a large tectonic event (e.g., the May 2008 Wenchuan earthquake) need to be further studied. Variations in the GPS velocity field, particularly the crustal strain field, can not only better describe the evolution of tectonic activity, but also characterize the present-day internal geodynamic mechanism of the region. Moreover, combining the overall motion with the local sub-block motion and the 3D crustal motion can more comprehensively reflect the regional dynamic environment.

In this study, we first use GPS horizontal velocities for different periods to investigate the variations of present-day crustal deformation of study region before and after the 2008 Wenchuan earthquake. Instead of using GPS horizontal velocity only to describe the general characteristics of crustal activity of the SETP within a certain time period, we also integrate the vertical velocity from leveling data and the horizontal velocity from GPS to analyze the three-dimensional (3D) differential crustal movement and sub-block activities. Second, considering that the crustal strain field could better reflect the response of the internal mechanism(s) of crustal deformation and reveal local strain accumulation rates and their possible correlation to seismicity, we further establish a sound strain model based on the least-squares collocation (LSC) technique, to overcome the observation errors in GPS data as well as sparseness and poor geometric distribution of the GPS data. Finally, based on our results and the regional crustal geodynamic, we discuss the correlation between the intensity of crustal activity and the strain rate distribution and the implication for the present-day geodynamic characteristics of the SETP.

2. Study area

The SETP is located in the transitional zone between the Tibetan Plateau and the SCB (Chen et al., 2013a), which is characterized by a steep topographic gradient and the South–North Seismic Zone of China (Xu et al., 2013) (Fig. 1). The region is tectonically active and shows strong crustal deformation, as well as markedly differential tectonic deformation patterns (Hao et al., 2014).

The SETP comprises a series of active faults, including the left-lateral Ganzi–Yushu–Xianshuihe and Anninghe–Zemuhe–Xiaojiang faults in the north and east, and the right-lateral Nujiang, Lijiang–Xiaojinhe, Lancangjiang, and Red River faults in the west and south (Hao et al., 2014; Ma et al., 1989) (Fig. 1). The strike-slip rates of these major faults have been studied through geological observations. The left-lateral strike slip rates of the Ganzi-Yushu, Xianshuihe, Anninghe, Zemuhe and Xiaojing faults are 12 ± 2.0 mm/yr, 14 ± 2.0 mm/yr, 6.5 ± 1.0 mm/yr, 6.4 ± 0.6 mm/yr, 10 ± 2.0 mm/yr, respectively (Song et al., 1998; Xu et al., 2003a,b). The right-lateral strike slip rates of the Lijiang–Xiaojinhe, Red River, Lancangjiang, Jinshajiang , Longriba and Longmenshan faults are 3.8 ± 0.7 mm/yr, 3.5 ± 1.5 mm/yr, 5.3 ± 1.1 mm/yr, 6.0 ~ 7.0 mm/yr, 5.4 ± 2.0 mm/yr, 1.5 ~ 2.0 mm/yr, respectively. (Ma et al., 2005; Zhou et al., 2006; Xu et al., 2003a,b, 2008, 2017). The occurrence of frequent earthquakes is also typically associated with these active faults. Historical earthquake records and paleoseismic data reveal that at least four strong earthquakes (M > 7) have occurred along the Ganzi–Yushu fault zone over the past ~700 years (Zhou et al., 1997a,b); approximately 20 earthquakes (M > 6) have occurred along the Xianshuihe fault since 1700 (Wen, 2000; Wen et al., 2008a); and almost 20 earthquakes (M > 6) have occurred along the Xiaojiang fault zone over the past 500 years (Shen et al., 2003; Song et al., 1998; Wen et al., 2008b; Xie and Cai, 1987). In

particular, on May 12, 2008, the most recent devastating seismic event (M 8.0 Wenchuan earthquake) occurred on the Longmenshan fault zone, which is located on the boundary between the Sichuan Basin and the SETP (Densmore et al., 2007). On April 14, 2010, another large earthquake (M 7.1 Yushu earthquake) occurred on the Ganzi-Yushu fault zone. These large earthquakes attest to the ongoing tectonic activity in the SETP.

In addition to the seismic activities, volcanism is frequent in the southwestern part of the study region (mainly around the Tengchong and Gengma areas). Geological and geophysical studies have shown that eruptions of intermediate–basic magma occurred around the southwestern Yunnan Province (Jiang, 1998; Wang et al., 2006), which were similarly controlled by tectonic faults (Chen et al., 1994; Wang and Huangfu, 2004; Yin and Harrison, 2000).

3. Method and data

The GPS data used in this paper were obtained from the China Crustal Movement Observation Network (CCMON) and the Earthquake Science Foundation of the China Earthquake Administration (CEA) (SMCCEA, 2013). The GPS horizontal velocity solutions are from the Second Monitoring and Application Center of the CEA, who processed the GPS data based on the methods used by Gan et al. (2007) and Wang (2009) (SMCCEA, 2013; Wang et al., 2013). GPS data are processed in 4 steps. First, the GAMIT software (King and Bock, 1995) was used to obtain loosely constrained daily solutions for satellite orbits and positions of regional stations. Second, the GLOBK software (Herring, 1998) was employed to combine the solutions with the daily loosely constrained solutions of the global IGS network produced by the SOPAC (http://sopac.ucsd.edu), and output the loosely constrained solutions for the station coordinates, polar motion, and satellite orbits with their full variance-covariance matrices. Third, station positions and velocities were estimated in the ITRF2005 reference frame (Altamimi et al., 2007) using the QOCA software (http://gipsy.jpl.nasa.gov/qoca/). Fourth, in order to clearly show the interior deformation within China, the velocity solution with respect to the ITRF2005 frame was transformed into that with respect to the stable Eurasia reference frame. Note that the coseismic effects of the April 2010 M 7.1 Yushu earthquake at relevant GPS stations are removed using the coseismic module in the Quasi-Observation Combination Analysis (QOCA) software package (Dong et al., 1998, 2006; Liang et al., 2013). As for the May 2008 M 8.0 Wenchuan earthquake, during the data processing the GPS observations from 1999 to 2011 are analyzed together. We find that the 2008 Wenchuan earthquake has a great impart on the GPS stations close to the epicenter. Therefore, the coseismic displacement model (e.g., Shen et al. 2009) is used to deduct the coseismic effects at these stations. However, even though the coseismic model is adopted, it cannot completely eliminate the coseismic displacement effects on GPS stations particularly adjacent to the Longmenshan fault. So the observed GPS data at stations located so close to the rupture zone are removed. On the other hand, the GPS observations in 2008 are limited and mainly distributed around the Longmenshan fault, and most of the GPS observations (after 2007) used in this paper started 2009. Hence, we divide the whole time period into two segments (1999–2007 and 2009–2011) to analyze the variations of the crustal deformation during the two periods (SMCCEA, 2013; Wang et al., 2013). The GPS horizontal velocity fields for the SETP in 1999–2007 and 2009–2011 are shown in Fig. 2a and b, respectively

The crustal GPS velocity field reflects only direct surface deformation. However, the strain rate field can not only numerically describe ongoing geodynamic processes, but also reflect the feedback mechanism of internal crustal deformation, as well as reveal local strain accumulation rates and their possible correlation to seismic hazard potential (Riguzzi et al., 2012). Thus, we further analyze the strain rate distribution in the region. Considering that observation errors in GPS data, as well as sparseness and poor geometric distribution of the data may result in a biased strain field, we use the least-squares collocation (LSC) technique to calculate the strain field by utilizing spatial interpolation and filtering based on a covariance function (Gaussian function) that describes the spatial correlation between any two observations (Jiang and Liu, 2010; Jiang et al., 2014; Qu et al., 2017; Wu et al., 2015a).

The LSC method is a stable and robust technique, since it minimizes the effect of human error in the calculation process. In this paper, the Gaussian functions $C(d) = C(0)\exp\{-k^2d^2\}$ (Jiang and Liu, 2010; Jiang et al., 2014; Qu et al., 2017; Wu et al., 2015a) for the 1999–2007 and 2009–2011 datasets are constructed with the parameters $C(0) = 18.13$ mm/yr^2 and $k = 0.0038$ km^{-2}, and $C(0) = 23.40$ mm/yr^2 and $k = 0.0037$ km^{-2}, respectively. The root-mean-square errors (RMSE) of the misfit to the GPS observations (between the observed and the LSC-predicted values) are $\sim$0.45 mm/yr, which is slightly smaller than the average error ($\sim$1.0 mm/yr) of the GPS velocity field, which indicates that the LSC method can describe the GPS velocity field well. More important, the reliability of the subsequent strain rate results depends on the quality of model fit to the GPS velocity. Therefore, the good fit between the observed and the LSC-predicted values could provide more reliable strain results. Therefore, the good fit between the observed and the LSC-predicted values could provide more reliable strain results. Thus, we employ the LSC technique to estimate the strain rate components in spherical coordinates, such as the principal strain rates, the maximum shear strain rate, and the plane strain gradient (Jiang and Liu, 2010; Jiang et al., 2014; Qu et al., 2017; Wu et al., 2011).

4. Result

The long-term horizontal velocity field, monitored from 1999 to 2007 (Fig. 2a), better reflects the overall tendency and spatial variation of the crustal motion. Fig. 2a shows that the GPS velocity field of the SETP displays clear spatial heterogeneity. The GPS velocity magnitude within the Tibetan Plateau is larger than that in the SCB. This indicates that the Tibetan Plateau experiences more intense crustal activity relative to its surrounding stable block. We also find that the GPS velocity near the Longmenshan fault, where the May 2008 M 8.0 Wenchuan earthquake occurred (Shen et al., 2009), was very small in 1999–2007 (Fig. 2a). The entire SETP shows an overall clockwise motion with respect to the stable Eurasian Plate, while the velocity decreases from north to south (below the Songpan–Ganzi Plateau). Taking the Lijiang–Xiaojinhe fault as the boundary, on both sides of the fault the GPS velocity directions are gradually deflected from SE to SSE. Taking the Red River fault as the boundary, the GPS velocity magnitudes on the south and west side of the fault are clearly smaller, and the directions are gradually deflected from SSE to S. The Nujiang fault, located in the southwestern part of the SETP, appears to play a particular role in shielding and absorption of the clockwise motion. The GPS velocity directions in this area rotate and trend toward the SSW. These GPS velocity characteristics are consistent with the regional neotectonic setting: the current crustal movement of the southwestern part of the SETP mainly exhibits clockwise rotation. This suggests that the present-day crustal deformation of the SETP is controlled by the northward compression of the Tibetan Plateau, resulting in eastward extrusion and clockwise rotation of the SETP around the Eastern Himalayas (Chen et al., 2013a,b; Royden et al., 2008; Wang et al., 2013; Wu et al., 2015b).

In contrast, the short-term velocity field, monitored during 2009–2011, reflects the variations in crustal motion after the Wenchuan earthquake (Fig. 2b). Although the overall crustal motion tendency is similar during the two different periods (Fig. 2a vs Fig. 2b), there are some local differences, particularly around the Longmenshan fault. The overall GPS velocity magnitude within the Tibetan Plateau increased in 2009–2011, while the SCB essentially maintained its original motion state. Thus, the differential movement between the SETP and the SCB is more obvious. Moreover, the magnitude of differential crustal motion

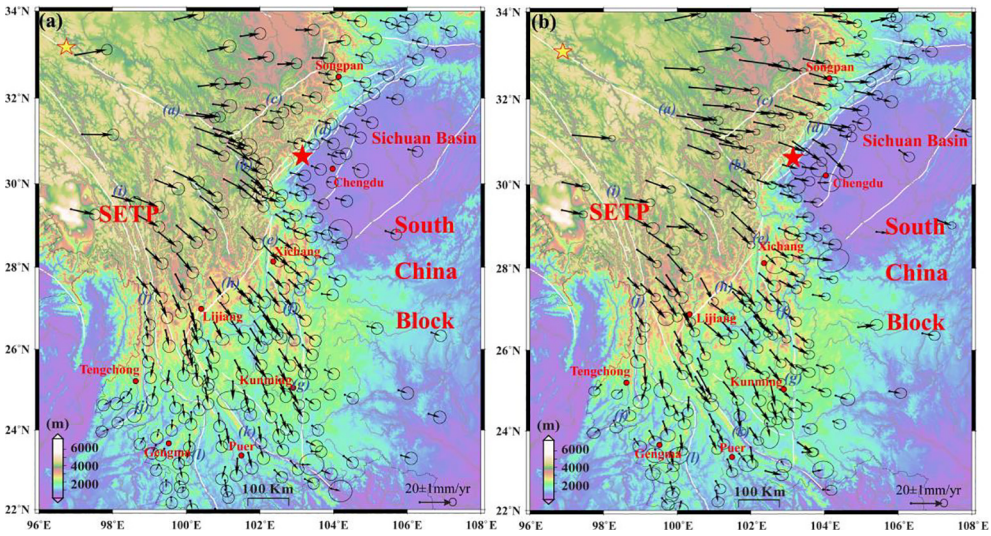

Fig. 2. The GPS velocities of the SETP and its surroundings for the periods of 1999–2007 (Fig. 2a) and 2009–2011 (Fig. 2b) (unit: mm/yr). Solid black arrows are GPS velocities with respect to the stable Eurasia plate based on ITRF2005 reference frame. The error ellipse represents the 95% confidence. The yellow star indicates the epicenter of the Yushu earthquakes.

on both sides of the Longmenshan fault increased significantly, which mainly reflect the post-seismic relaxation caused by the Wenchuan earthquake (Wang, 2010).

Crustal motion and deformation show large spatial–temporal scale characteristics during the build-up and occurrence of large earthquakes, which is closely related to the regional 3D differential crustal movement. Therefore, integrating the horizontal and vertical crustal velocities has significant reference value for understanding the present-day geodynamics of the SETP. The horizontal crustal velocities are obtained from the large-scale GPS observations (Fig. 2a and b), and the background vertical motion field is obtained from long-term leveling data (1970s–2011) (Hao et al., 2014). In order to obtain a more comprehensive regional 3D crustal motion image, the GPS horizontal velocities are superimposed on the continuous vertical velocities (Fig. 3a and b).

The 3D crustal velocities reflect significant differences in the tectonic activity of different structural belts (Fig. 3a and b). The Songpan–Ganzi Plateau shows overall uplift, and the middle and northern areas of the Sichuan–Yunnan block also show uplift while the southern part shows subsidence. In particular, the regions undergoing intense horizontal crustal shortening (Fig. 2a and b) are the ones that exhibit significant vertical uplift, such as the eastern area of the Songpan–Ganzi Plateau and the northeastern area of the Sichuan–Yunnan block (yellow and red areas in Fig. 3a and b). Basins characterized by horizontal tension (Fig. 2a and b) show clear vertical subsidence (Fig. 3a and b), such as in the southern area of the Sichuan–Yunnan block. These characteristics reflect the present-day geodynamics of the SETP, where shortening of the crust results in uplift of the mountain areas, while the basins show extensional subsidence (Hao et al., 2014; Wang et al., 2013).

In order to more comprehensively reflect the regional geodynamic environment, the detailed activities of the local sub-blocks are further studied on the basis of the overall motion and deformation framework. Thus, the SETP and its surrounding area are divided into six sub-blocks based on the distribution of tectonic faults, the GPS velocity results, and the crustal motion characteristics (Hao et al., 2014; Wang, 2009) (Fig. 4a and b). We then calculate the horizontal crustal velocity fields and the principal strain rates for each sub-block using the block kinematic model (Qu, 2008) based on the horizontal GPS velocity fields (Fig. 2a and b). The overall sub-block crustal movements are toward the southeast, with lateral slip and clockwise rotation characteristics (Fig. 4a and b). These features are consistent with the results of geological studies (Xu et al., 2003a,b) and seismic moment tensor inversion (Ding, 2010), which indicate that the eastward extrusion of the Tibetan Plateau is absorbed and adjusted through tectonic faults rather than by rapid lateral escape along a few large strike-slip faults (Shen et al., 2005; Zhu et al., 2017).

During the period 2009–2011, all of the sub-block motion directions were deflected toward the east, accompanied by increased velocity

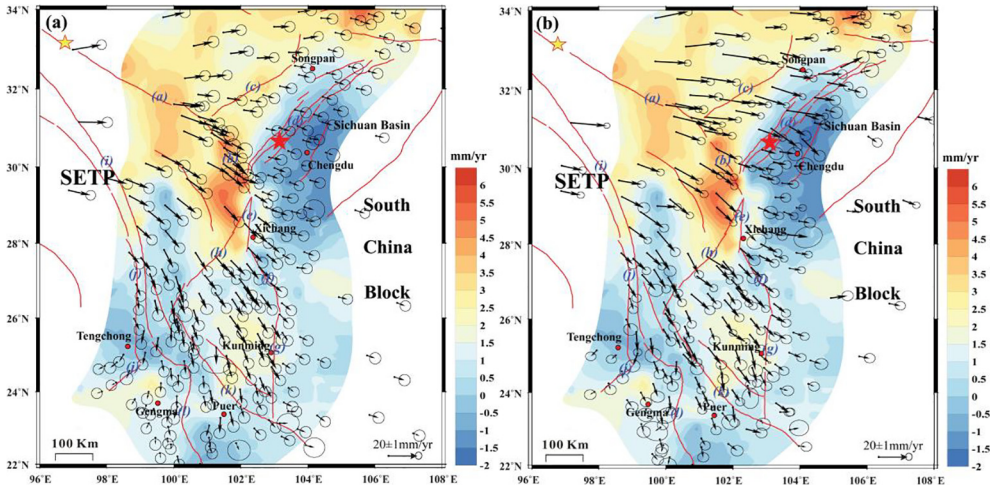

Fig. 3. The 3D crustal velocity fields over the SETP region, during the periods of 1999–2007 (Fig. 7a) and 2009–2011 (Fig. 7b). The color bar represents the vertical velocities from the long time scale leveling data (Hao et al., 2014).

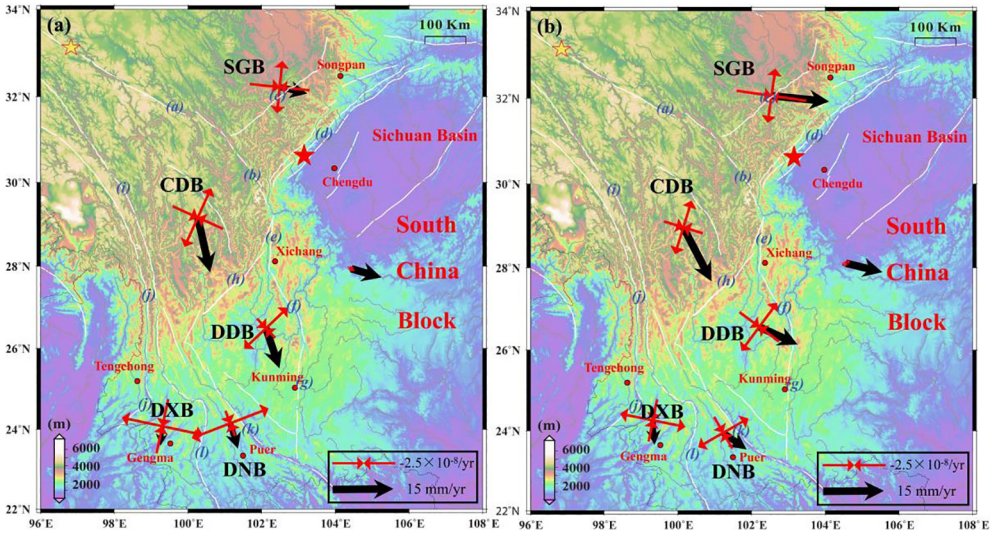

Fig. 4. The horizontal velocity fields and the principal strain rates of each sub-block calculated by the block kinematic model, during the periods of 1999–2007 (Fig. 6a) and 2009–2011 (Fig. 6b). Abbreviations are: SGB, the Songpan-Ganzi sub-block; CDB, the Chuandian sub-block; DDB, the Diandong sub-block; DNB, the Diannan sub-block; DXB, the Dianxi sub-block. The red cross arrows indicate the principal strain rate vectors of each sub-block. The length and the direction of the arrow represent the same features as they do in Fig. 3 caption. The bold black arrows are the horizontal velocity fields of each sub-block.

magnitudes (Fig. 4a vs Fig. 4b). On the Songpan–Ganzi Plateau in particular, the crustal velocity magnitude increased significantly. The principal strain rates of the boundary blocks also changed considerably in 2009–2011 (Fig. 4a vs Fig. 4b): the compressional strain rate in the nearly E–W direction on the Songpan–Ganzi Plateau experienced marked increase, and the compressional strain rates in the nearly NW–SE direction of the Diandong and the Diannan blocks also increased. In contrast, the principal strain rate magnitudes of the SCB remained very small during the two different periods, which is consistent with the crustal stiffness characteristics of the SCB block (Zhu et al., 2006). According to the above-mentioned variation characteristics of the crustal velocity and principal strain rate fields, we infer that the variation of the sub-block crustal activities may also have been affected by the occurrence of the Wenchuan earthquake.

Vector maps of the principal strain rates for the periods 1999–2007 and 2009–2011 are shown in Fig. 5a and b, respectively. Fig. 5a shows that significant compressional strain rates mainly occur along the tectonic boundary belts between the SETP and the SCB, accompanied by associated extensional strain. The Ganzi–Yushu–Xianshuihe fault zone show the highest compressional strain rate values (approximately -3×10^{-8}/yr) in the E–W direction, accompanied by extensional strain in the N–S direction. In addition, the Anninghe–Zemuhe–Xiaojiang fault zone show relatively high compressional strain rates (approximately -2.4×10^{-8}/yr) in the NWW-SNN direction, accompanied by extensional strain in the NNE–SSW direction. The Lijiang–Xiaojinhe fault, the Red River fault, and the western and southern areas of Yunnan Province also show high principal strain rate values. Of these areas, the Lijiang–Xiaojinhe fault, the Red River fault, and the southern Yunnan Province show compressional strain oriented in the nearly N–S direction, accompanied by extensional strain in the nearly E–W direction. However, the western areas of Yunnan Province show compressional strain oriented in the nearly NE–SW direction, accompanied by extensional strain in the nearly NW-SE direction. Importantly, it should be noted that the principal strain rate values around the Longmenshan fault zone were very small in 1999–2007, which is consistent with previously published results (Wu et al., 2015a). The spatial characteristics of the principal strain fields are similar for the two different periods (Fig. 5a vs Fig. 5b); that is, significant principal strain rates are mainly concentrated on the tectonic boundary belts between the SETP and the SCB, particularly along the tectonic fault zones. However, several differences in the principal strain rates exist between the two different periods. Comparing Fig. 5b with Fig. 5a, we can clearly see a significant compressional strain rate around the Longmenshan fault area, oriented in the NW–SE direction with a mean strain rate of up to approximately -5×10^{-8}/yr, which indicates that the strain state in this area may have been affected by the occurrence of the Wenchuan earthquake. Moreover, during the period 2009–2011, the compressional strain rate directions along the Ganzi–Yushu–Xianshuihe fault zone are slightly deflected to the southeast (Fig. 5a vs Fig. 5b). The compressional strain rates increased

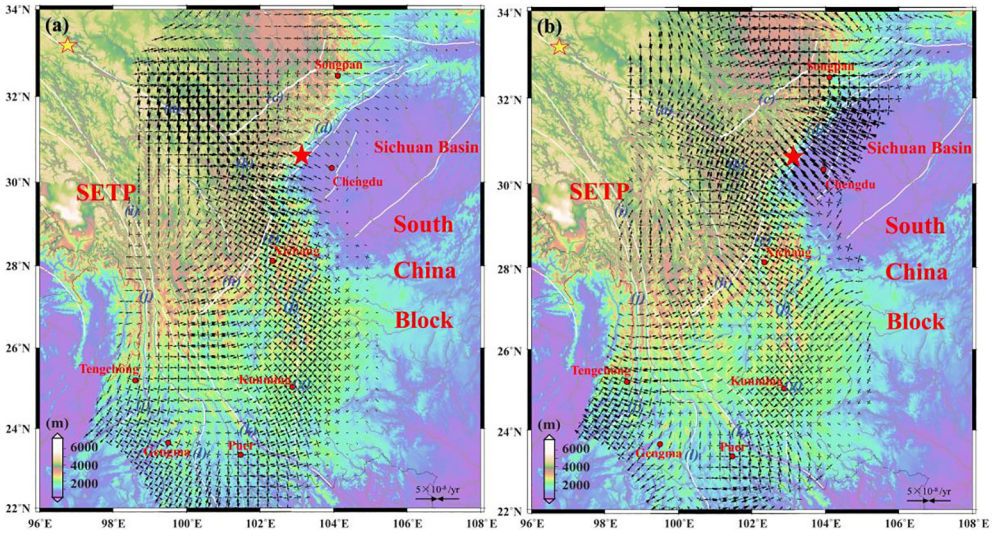

Fig. 5. The distribution characteristics of the principal strain rates of the SETP and its surroundings for the periods of 1999–2007 (Fig. 3a) and 2009–2011 (Fig. 3b) (unit: 10^{-8}/yr). The black cross arrows indicate the principal strain rate vectors. The length and the direction of the arrow represent the magnitude and the principal direction of the principal strain rate. The opposing arrow represents the extensional principal strain rate, while the relative arrow represents the compressional principal strain rate.

around the Lijiang–Xiaojinhe and the Anninghe faults (Fig. 5a vs Fig. 5b), which is consistent with the conclusion of Wan et al. (2009) that the variations of crustal movement along the eastern boundary of the Sichuan–Yunnan block are mainly influenced by the Wenchuan earthquake. Especially, the postseismic effect of the earthquake may be the primary factor to affect the regional strain field by strengthening the strain accumulation. Additionally, the compressional strain rates around the Red River fault and the southern areas of Yunnan Province also increased during the period 2009–2011, while the extensional strain rates in the western areas of Yunnan Province increased (Fig. 5a vs Fig. 5b).

Further, the overall principal strain rate distribution characteristics obtained in this paper are also consistent with the present-day geodynamic setting of the region. The crustal deformation of the SETP is mainly influenced by the nearly eastward extrusion of the Tibetan Plateau block (Bai et al., 2010; Liu et al., 2007; White and Lister, 2012), with resistance from the SCB to the eastward expansion of the Tibetan Plateau causing lateral extrusion of the crustal materials toward the southeast (Yao et al., 2010). Therefore, the tectonic boundary belts between the SETP and the SCB present relatively significant compressional strain rates, accompanied by associated extensional strain.

The maximum shear strain rate distributions are also constructed to analyze the intensity of crustal activity in the SETP (Fig. 6a and Fig. 6b). Since the shear strain rate magnitude reflects the degree of crustal deformation; the higher the shear strain rate, the more intense the crustal activity (Segall, 2010). High maximum shear strain rate values are mainly concentrated on the tectonic boundary belts between the SETP and the SCB (Fig. 6a and b). The most striking difference is observed in the Longmenshan fault area, which was characterized by low maximum shear strain rate values in 1999–2007 (Fig. 6a); this same area showed the highest maximum shear strain rates in 2009–2011 (Fig. 6b), with maximum values of up to approximately 6×10^{-8}/yr. This further indicates that the crustal activity around the Longmenshan fault area may have been significantly affected by the occurrence of the Wenchuan earthquake. In contrast, the Ganzi–Yushu–Xianshuihe fault shows high maximum shear strain rate values during the two different periods (Fig. 6a and b); a similar situation can be observed along the Anninghe–Zemuhe–Xiaojiang, Lijiang–Xiaojinhe, and Red River faults, as well as the western and southern Yunnan Province. These characteristics indicate that the tectonic boundary belts between the SETP and the SCB accommodate intense present-day crustal activity (Densmore et al., 2007; Shen et al., 2003; Wen et al., 2008a, 2008b).

Fig. 7a and b show that the transition zones of the high and low plane strain gradients are also concentrated on the boundary between the SETP and the SCB, particularly along the Ganzi–Yushu–Xianshuihe, Anninghe–Zemuhe–Xiaojiang, Lijiang–Xiaojinhe, and Red River faults, as well as the western and southern Yunnan Province. Transition zones showing large spatial variations in plane strain gradients indicate a higher likelihood of strong earthquakes, which can be used for medium- to long-term earthquake prediction in specific areas (Qu et al., 2017; Zhang et al., 2013a).

5. Discussion

Comparing Fig. 6b with Fig. 6a, we can see that there is an obvious decrease in the maximum shear strain rates along the Ganzi-Yushu fault. In contrast, the maximum shear strain rates increased significantly adjacent to the Longriba fault at the Songpan-Ganzi plateau. The maximum shear strain rates along Ganzi-Yushu fault (southeastern segment) decrease significantly after the 2008 Wenchuan earthquake (Fig. 6b versus Fig. 6a). This suggests that the Ganzi-Yushu fault has locked and accumulated shear strain intensively before 2008. Due to the occurrence of Wenchuan earthquake, the accumulated strain along the Ganzi-Yushu fault has been released and its seismic hazard will be reduced accordingly. However, this phenomenon only was present in a shorter period of time (2009–2011). According to the chain reaction principle of strong earthquake activity (e.g., Matsuda, 1981), the seismic activity usually has some sort of triggering or cause changes in the stress regime at different segments of a large fault system. When a large earthquake occurs in one of the segments, the rapid sliding of blocks on both sides of this segment will have impact on the stress state in other segments of the fault and can cause the adjacent segments to be the dangerous area for the next earthquake. For example, 7 years after the 1920 M 8.5 earthquake in Haiyuan fault, the 1927 M 8.0 Gulang earthquake occurred along the adjacent Qilianshan fault (Wu et al., 2014). Therefore, considering that the 2010 M 7.0 Yushu earthquake occurred in the northwestern segment of the Ganzi-Yushu fault, the southeastern segment of the Ganzi-Yushu fault should be drawn more attention in the future (Gu et al., 1983; Zhou et al., 1997a,b; Wen et al., 2003).

The maximum shear strain rates along the Longriba fault increased greatly after the Wenchuan earthquake (Fig. 6b versus Fig. 6a). The result indicates that the shear strain energy along the northern segment of the Longriba fault is accumulating and the potential seismic risk increases accordingly. Moreover, the Longriba fault zone is a seismic gap without large recorded earthquakes (Xu et al., 2008), and according to the principle of seismic gap it should be the risky area of strong earthquakes in the future (Slemmons and Depolp, 1986; Wu et al., 2014). Considering that the 2010 M 7.0 Yushu and 2008 M 8.0 Wenchuan earthquakes have taken place around the Longriba fault, the active fault should also be drawn more attention in the future. On the other hand, because of the high strain accumulation in the northern

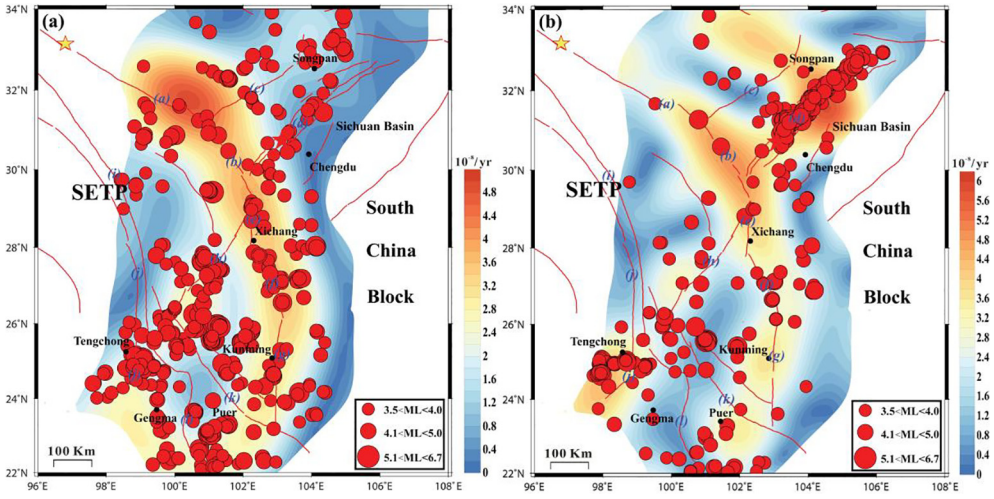

Fig. 6. The distribution characteristics of maximum shear strain rates (unit: 10^{-8}/yr) and the distribution of earthquakes (different sizes of the red solid circles) over the SETP region, during the periods of 1999–2007 (Fig. 4a) and 2009–2011 (Fig. 4b). The red solid lines represent the major active faults (Zhang et al., 2005). The seismic statistical records are from the second high-tech research center monitoring room of the China Seismological Bureau.

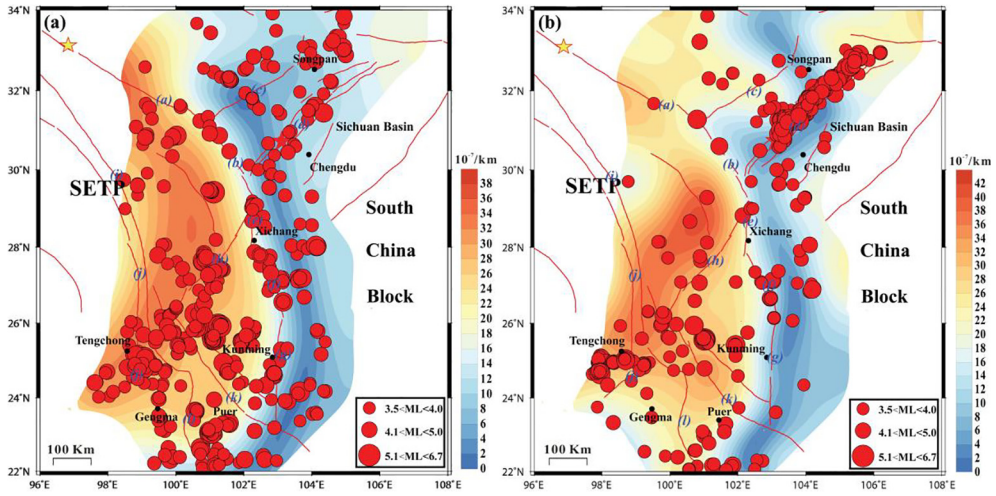

Fig. 7. The distribution characteristics of plane strain gradient (unit: 10^{7}/km) and the distribution of earthquakes over the SETP region, during the periods of 1999–2007 (Fig. 5a) and 2009–2011 (Fig. 5b).

segment of the Longriba fault, it is more sensitive to the disturbance of large earthquakes in the surrounding area. As a matter of fact, after the 2017 Jiuzhaigou earthquake, the shear strain rates along the northern Longriba fault did not show a reduction, which implies high seismic risk (Xu et al., 2017). We should keep on paying close attention to the crustal movement along the Longriba fault.

In addition, significant variations in the horizontal crustal velocity around the Longmenshan fault zone reflects the influence of the postseismic relaxation of the Wenchuan earthquake (Fig. 2b versus Fig. 2a). The postseismic effect is mainly caused by the viscoelastic relaxation process driven by the lower crust and upper mantle after the Wenchuan earthquake (Bai et al., 2010). Moreover, the postseismic effect can control the long-term distribution of the crust stress field (Rice and Gu, 1983; Pollitz et al., 2001; Xiong et al., 2010). Therefore, the postseismic relaxation of the Wenchuan earthquake will have a long-term impact on the crustal movement around the Longmenshan fault zone (Wang, 2010).

The changes in the strain field around the Longmenshan fault further clearly reflect the postseismic effect of the Wenchuan earthquake (Figs. 5 and 6). In addition, some related studies have shown that there still is an obviously low velocity anomaly under the earthquake source area of Wenchuan, which may play a role in the accumulation of the strain energy (Lei et al., 2009). Moreover, the regional strain field in 2009–2011 also shows that the strain field mainly presents the compressional strain rate in the NW–SE direction, which indicates that the lateral compressional stress region is still dominant. Hence, the strain accumulation rate around the Longmen mountain fault zone continues. When the accumulated strain energy exceeds a critical value, the fault will releases the accumulative energy to maintain the balance of the fault system. The 2013 M 7.0 Lushan earthquake in the southern segment of the Longmenshan fault was an example that occurred after the Wenchuan earthquake (Zou et al., 2015).

On the other hand, Segall (2010) study shows the magnitude of shear strain rate reflects the degree of crustal deformation; that is, the higher the shear strain rate, the more intense the crustal activity. Furthermore, higher rates of strain accumulation should generally be associated with larger or more frequent earthquakes. In addition, the transition zones of the significant plane strain gradients indicate strain accumulation in these fault zones, which are therefore hazardous areas where earthquakes are likely to occur (Zhang et al., 2013a). Indeed, we find that earthquakes occurred more frequently on the tectonic boundary belts between the SETP and the SCB, particularly along the Ganzi–Yushu–Xianshuihe, Anninghe–Zemuhe–Xiaojiang, Lijiang–Xiaojinhe, and Red River faults, as well as in the western and southern Yunnan Province (Fig. 6a and b). Importantly, the variations in maximum shear strain and the transition zones of the significant plane strain gradients all indicate that the strain rates around the Longmenshan fault area changed considerably in 2009–2011, which is also consistent with the changes in earthquake distribution around the fault areas (Fig. 7b vs Fig. 6b). We infer that the variations in strain rates and earthquake distribution around the Longmenshan fault zone were mainly caused by the occurrence of the Wenchuan earthquake.

Forming part of the broad accommodation zone that absorbs the deformation induced by the collision and continuous convergence of the Indian and Eurasian plates, the SETP deformation is accommodated by complex internal tectonic deformation, southeastward crustal extrusion, and rotation (Yin and Harrison, 2000). Due to the resistance from the SCB to the eastward expansion of the Tibetan Plateau, lateral extrusion of the crustal materials to the southeast results in upper crustal clockwise rotation around the eastern Himalayan syntaxis (Figs. 2 and 3) and significant compressional strain rates along the tectonic boundary belts between the SETP and the SCB (Fig. 5a and b).

In addition to the upper crustal deformation and rotation, lower crustal flow preferentially accommodates the internal deformation within the Songpan–Ganzi Plateau and the Sichuan–Yunnan block (Chen et al., 2013a,b), such that these blocks are mainly characterized by long-term vertical uplift (Fig. 3a and b). Zhang (2008) further considered that the lower crust underlying the Sichuan–Yunnan block deforms by plastic flow, while that of the Sichuan Basin and the SCB does not. This plastic flow drives the upper crustal deformation and fault activities, which leads to strain accumulation and release on the faults, producing frequent earthquakes. In contrast, the eastward subduction of the Indian Plate below the Burma Arc induces back-arc spreading in the upper plate, causing the southern and western Yunnan Province to be characterized mainly by nearly southwestward motion (Fig. 2a and b) and E–W extension (Fig. 5a and b) (Wang et al., 2008; Wang et al., 2015).

It should be noted that the GPS data predominantly record interseismic strain patterns; a precondition is that one must know where the GPS-predicted strain will be released. Therefore, the deformation signal of the region of intense tectonic activity can be more easily interpreted using the LSC strain calculation method based on long-term GPS data (Jiang and Liu, 2010; Jiang et al., 2014; Qu et al., 2017; Wu et al., 2011). The dynamic adjustment for a few years or short-term GPS data may affect the decipherable process (Wu et al., 2015a). Fortunately, since sufficient deformation and strain variations occurred in the SETP during 2009–2011, several important deformation signals can be interpreted. Furthermore, we analyzed the intensity of crustal activity

based mainly on small-earthquake activities. However, the intensity may additionally be related to volcanic activity, such as in the southwestern Yunnan Province. In addition, we analyzed the correlation between the seismicity distribution and the maximum shear strain rates or the transition zones of the significant plane strain gradients based mainly on the degree of crustal activity. In fact, the development and occurrence of earthquakes are complex. Besides the small-earthquake distribution records used in this paper, more detailed seismic data will be useful to analyze the coulomb stress change. Moreover, although the main postseismic displacements of the Wenchuan earthquake were mainly concentrated within ~50 days after the main shock and decayed rapidly with distance (Cui et al., 2016; Ding et al., 2013), this will inevitably have a specific impact on the regional crustal activities. In contrast, considering long-term geodynamic processes, the GPS observations reflect the present-day crustal deformation activity, which represents only a brief moment compared to geologic timescales. Therefore, in future work, we will combine longer-timescale GPS observations and geophysical monitoring data with additional large-scale InSAR or Gravity Recovery and Climate Experiment (GRACE) satellite observations to further explore the mechanism(s) of crustal deformation and the geodynamic processes in the SETP and surrounding areas.

6. Conclusion

Based on large-scale GPS observations in the SETP and surrounding areas, we obtain the present-day crustal deformation characteristics, which can provide a wide range of quantitative spatial information for regional tectonics, as well as insights into the kinematic and geodynamic processes in this region.

The entire SETP shows overall clockwise rotation around the eastern Himalayan syntaxis. The 3D velocity fields further reflect significant differences in tectonic activity between different structural belts: the regions undergoing intense horizontal crustal shortening are characterized by significant vertical uplift; in contrast, the basins displaying horizontal tension show clear vertical subsidence.

Significant compressional strain rates are mainly concentrated along the tectonic boundary belts between the SETP and the SCB, accompanied by associated extensional strain rates. Relatively high maximum shear strain rates and the transition zones of the significant plane strain gradients are also mainly concentrated along the Ganzi–Yushu–Xianshuihe, Anninghe–Zemuhe–Xiaojiang, Lijiang–Xiaojinhe, and Red River faults, as well as the western and southern Yunnan Province. This indicates intense crustal activity in these regions, which is consistent with the spatial distribution of earthquakes.

The crustal deformation characteristics obtained in this study are consistent with present-day geodynamic settings, as well as geological and geophysical results. Furthermore, according to the variation characteristics of the crustal deformation and strain fields, we infer that the present-day crustal motion and deformation of the SETP are principally influenced by the nearly eastward extrusion of the Tibetan Plateau, with resistance from the SCB to the eastward expansion of the Tibetan Plateau causing lateral extrusion of the crustal materials to the southeast. It should be noted that around the Longmenshan fault area, the crustal velocity and strain rate values from 1999 to 2007 are all small; in contrast, values for 2009–2011 increased significantly, which is consistent with the sub-block activity characteristics. This also indicates that the variations in crustal deformation around the Longmenshan fault are mainly related to the occurrence of the Wenchuan earthquake.

Acknowledgements

The authors are grateful to surveyors who work hard around the southeastern Tibetan Plateau in a challenging environment to obtain GPS data. We thank the second high-tech research center monitoring room of China Seismological Bureau for providing the high precision GPS data. This study is also supported by the Nature Science Fund of China (NSFC) (project Nos: 41674001, 41731066, 41790445, 41604001, 41504005, 41202189), the Natural Science Basic Research Plan in Shaanxi Province of China (project No. 2016JM4005), the Special Fund for Basic Scientific Research of Central Universities (No. CHD300102268204), the Earthquake Science Foundation of CEA (project No: 201208009), and the China Postdoctoral Science Foundation (project Nos: 2013M530412, 2016M602741). Some Figures were prepared using the public domain Generic Mapping Tools GMT (Wessel and Smith, 1998). Constructive comments from three anonymous reviewers and the editor improved the manuscript.

References

Altamimi, Z., Collilieux, X., Legrand, J., et al., 2007. ITRF2005: a new release of the international terrestrial reference frame based on time series of station positions and earth orientation parameters. J. Geophys. Res.-Solid Earth 112 (B9), B9401.

Bai, D.H., Unsworth, M.J., Meju, M.A., Ma, X.B., Teng, J.W., Kong, X.G., Sun, Y., Sun, J., Wang, L.F., Jiang, C.S., Zhao, C.P., Xiao, P.F., Liu, M., 2010. Crustal deformation of the eastern Tibtan plateau revealed by magnetotelluric imaging. Nat. Geosci. 3 (5), 358–362.

Cai, Y., Wu, J.P., Fang, L.H., Wang, W.L., Yi, S., 2016. Crustal anisotropy and deformation of the southeastern margin of the Tibetan Plateau revealed by Pms splitting. J. Asian Earth Sci. 121, 120–126.

Chang, L.J., Ding, Z.F., Wang, C.Y., Flesch, L.M., 2017. Vertical coherence of deformation in lithosphere in the NE margin of the Tibetan plateau using GPS and shear-wave splitting data. Tectonophysics 699, 93–101.

Chen, L., Gerya, T., Zhang, Z.G., Zhu, G.Z., Duretz, T., Jacoby, W.R., 2013a. Numerical modeling of eastern Tibetan-type margin: influences of surface processes, lithospheric structure and crustal rheology. Gondwana Res. 24, 1091–1107.

Chen, Q., Yang, Y.H., Luo, R., Liu, G.X., Zhang, K., 2015. Deep coseismic slip of the 2008 Wenchuan earthquake inferred from joint inversion of fault stress changes and GPS surface displacements. J. Geodyn. 87, 1–12.

Chen, X., Li, J., Zhao, J., 1994. The basement structural characteristic of sanjiang structure belt and its relationship with strong earthquakes. In: Chen, Y.T., Kan, R.J., Teng, J.W. (Eds.), Advances in Solid Earth Geophysics in China. Oceanic Press, Beijing, pp. 41–54 (in Chinese).

Chen, Y., Zhang, Z.J., Sun, C.Q., Badal, J., 2013b. Crustal anisotropy from Moho converted Ps wave splitting analysis and geodynamic implications beneath the southeastern margin of Tibet and surrounding regions. Gondwana Res. 24, 946–957.

Cui, D.X., Hao, M., Li, Y.H., Wang, W.P., Qing, X.L., Li, C.J., 2016. Present-day crustal movement and strain of the surrounding area of Ordos block derived from repeated GPS observations. Chin. J. Geophys. 59 (10), 3646–3661 (in Chinese with English abstract).

Densmore, A.L., Ellis, M.A., Li, Y., Zhou, R.J., Hancock, G.S., Richardson, N., 2007. Active tectonics of the Beichuan and Pengguan faults at the eastern margin of the Tibetan Plateau. Tectonics 26.

Ding, K.H., 2010. Research on present-day crustal deformation of central and east Qinghai-Tibet plateau. PhD thesis. Wuhan: Wuhan University (in Chinese with English abstract).

Ding, K.H., Xu, C.J., Wen, Y.M., 2013. Postseismic deformation associated with the 2008 Wenchuan earthquake by GPS data. Geomatics Informat. Sci. Wuhan Univ. 38 (2), 131–135 (in Chinese with English abstract).

Dong, D., Herring, T., King, R., 1998. Estimating regional deformation from a combination of space and terrestrial geodetic data. J. Geod. 72, 200–214.

Dong, D., Fang, P., Bock, Y., Webb, F., Prawirodirdjo, L., Kedar, S., Jamason, P., 2006. Spatiotemporal filtering using principal component analysis and Karhunen-Love expansion approaches for regional GPS network analysis. J. Geophys. Res. 111, B03405.

Fu, B.H., Shi, P.L., Guo, H.D., Okuyama, S., Ninomiya, Y., Wright, S., 2011. Surface deformation related to the 2008 Wenchuan earthquake, and mountain building of the Longmen Shan, eastern Tibetan Plateau. J. Asian Earth Sci. 40, 805–824.

Gan, W.J., Zhang, P.Z., Shen, Z.K., Niu, Z.J., Wang, M., Wan, Y.G., Zhou, D.M., Cheng, J., 2007. Present-day crustal motion within the Tibetan Plateau inferred from GPS measurements. J. Geophys. Res. 112, B08416.

Gu, G.X., Lin, T.H., Shi, Z.L., et al., 1983. Catalogue of Chinese earthquakes (1831 BC to 1969 AD). Science Press, Beijing (in Chinese).

Hao, M., Wang, Q.L., Shen, Z.K., Cui, D.X., Ji, L.Y., Li, Y.H., Qin, S.L., 2014. Present day crustal vertical movement inferred from precise leveling data in eastern margin of Tibetan Plateau. Tectonophysics 632, 281–292.

He, J.K., Xia, W.H., Lu, S.J., Qian, H.S., 2011. Three-dimensional finite element modeling of stress evolution around the Xiaojiang fault system in the southeastern Tibetan plateau during the past ~500 years. Tectonophysics 507, 70–85.

Herring, T., 1998. GLOBK: Global Kalman filter VLBI and GPS analysis program, version 4.1, Mass. Inst. of Technol., Cambridge.

Jiang, G.Y., Xu, C.J., Wen, Y.M., Xu, X.W., Ding, K.H., Wang, J.J., 2014. Contemporary tectonic stressing rates of major strike-slip faults in the Tibetan Plateau from GPS observations using Least-Squares Collocation. Tectonophysics 615–616, 85–95.

Jiang, C., 1998. Distribution characteristics of Tengchong area, Yunnan province. J. Seismol. Res. 8, 107–120 (in Chinese).

Jiang, W.L., Zhang, J.F., Tian, T., Wang, X., 2012. Crustal structure of Chuan-Dian region derived from gravity data and its tectonic implications. Physics of the Earth and Planetary Interiors, 212–213:76–87 Tectonophysics 491, 205–210.

Jiang, Z.S., Liu, J.N., 2010. The method in establishing strain field and velocity field of

crustal movement using least squares collocation. Chinese. J. Geophys. 53 (5), 1109–1117 (in Chinese with an English abstract).
King, R., Bock, Y., 1995. Documentation of the GAMIT GPS analysis software, version 9.3, Mass. Inst. of Technol., Cambridge.
Lei, J.S., Zhao, D.P., Su, J.R., et al., 2009. Fine seismic Strueture under the Longmenshan fault zone and the meehanism of the large Wenehuanearthquake. Chinnese J. GeoPhys. (inChinese) 52 (2), 339–345.
Li, M.K., Zhang, S.X., Wang, F., Wu, T.F., Qin, W.B., 2016a. Crustal and upper-mantle structure of the southeastern Tibetan Plateau from joint analysis of surface wave dispersion and receiver functions. J. Asian Earth Sci. 117, 52–63.
Li, Y.C., Shan, X.J., Qu, C.Y., Wang, Z.J., 2016b. Fault locking and slip rate deficit of the Haiyuan-Liupanshan faultzone in the northeastern margin of the Tibetan Plateau. J. Geodyn. 102, 47–57.
Liang, S.M., Gan, W.J., Shen, C.Z., Xiao, G.R., Liu, J., Chen, W.T., Ding, X.G., Zhou, D.M., 2013. Three-dimensional velocity field of present-day crustal motion of the Tibetan Plateau derived from GPS measurements. J. Geophys. Res. Solid Earth 118, 1–11.
Lin, A.M., Rao, G., Jia, D., Wu, X.J., Yan, B., Ren, Z.K., 2011. Co-seismic strike-slip surface rupture and displacement produced by the 2010 MW 6.9 Yushu earthquake, China, and implications for Tibetan tectonics. J. Geodyn. 52, 249–259.
Lin, A.M., Rao, G., Yan, B., 2014. Structural analysis of the right-lateral strike-slip Qingchuan fault, northeastern segment of the Longmen Shan thrust belt, central China. J. Struct. Geol. 68, 227–244.
Liu, C., Zhu, B.J., Yang, X.L., 2015. How does crustal shortening contribute to the uplift of the eastern margin of the Tibetan Plateau? J. Asian Earth Sci. 98, 18–25.
Liu, C., Zhu, B.J., Yang, X.L., Shi, Y.L., 2016. Phys. Earth Planet. Inter. 252, 23–36.
Liu, M., Yang, Y.Q., Shen, Z., Wang, S., Wang, M., Wan, Y., 2007. Active tectonics and intra-continental earthquakes in China: The kinematics and geodynamics. In: Stein, S., Mazzotti, S., (Eds.), Continental Intraplate Earthquakes: Science, Hazard, and Policy Issues: Geological Society of America Special Paper 425, 299–318.
Liu, Y., Xu, C.J., Li, Z.H., Wen, Y.M., Forrest, D., 2011. Interseismic slip rate of the Garze-Yushu fault belt in the Tibetan Plateau from C-band InSAR observations between 2003 and 2010. Adv. Space Res. 48, 2005–2015.
Ma, X.Y., Ding, G.Y., Zhang, H.G., Zhang, B.C., Ma, Z.J., 1989. Lithospheric Dynamics Atlas of China. China Cartographic Publishing House, pp. 1-68 (in Chinese).
Ma, B.Q., Su, G., Hou, Z.H., et al., 2005. Late quaternary slip rate in the central part of the Longmenshan fault zone from terrace deformation along the Minjiang river. Seismol. Geol. (in Chinese) 27 (2), 234–242.
Matsuda, T., 1981. Active faults and damaging earthquakes in Japan macroseismic zoning and precaution fault zones. Maurice Ewing Series 4, 279–289.
Pollitz, F.F., Wicks, C., Thatcher, W., 2001. Mantle flow beneath a continental strike-slip fault: postseismic deformation after the 1999 Hector Mine earthquake. Science 293 (5536), 1814–1818.
Qu, W., 2008. The deformation characteristic of the northeastern marginof Qinghai-Tibet plateau Constrained by GPS observations (Master Thesis), Chang'an University (in Chinese).
Qu, W., Lu, Z., Zhang, M., Zhang, Q., Wang, Q.L., Zhu, W., Qu, F.F., 2017. Crustal strain fields in the surrounding areas of the Ordos Block, central China, estimated by the least-squares collocation technique. J. Geodyn. 106, 1–11.
Riguzzi, F., Crespi, M., Devoti, R., Doglioni, C., Pietrantonio, G., Pisani, A.R., 2012. Geodetic strain rate and earthquake size: new clues for seismic hazard studies. Phys. Earth Planet. Inter 206–207, 67–75.
Rice, J.R., Gu, J.C., 1983. Earthquake aftereffects and triggered seismic phenomena. Pure Appl. Geophys. 121 (2), 187–219.
Robert, A., Zhu, J., Vergne, J., Cattin, R., Chan, L.S., Wittlinger, G., Herquel, G., Sigoyer, J.D., Pubellier, M., Zhu, L.D., 2010. Crustal structures in the area of the 2008 Sichuan earthquake from seismologic and gravimetric data.
Royden, L.H., Burchfiel, B.C., van der Hilst, R.D., 2008. The geological evolution of the Tibetan Plateau. Science 321, 1054–1058.
Second Monitoring Center, China Earthquake Administration (SMCCEA), 2013. China comprehensive geophysical field observation – Project of the surrounding areas of the Ordos block (Xi'an, Shaaxi province, China (in Chinese).
Segall, P., 2010. Earthquake and Volcano Deformation. Princeton University Press, New Jersey/Oxfordshire.
Slemmons, D.B., Depolp, C.M., 1986. Evaluation of active faulting and associated hazards. In: Wallace, Robert E. (Ed.), Active tectonics. National Academy Press, Washington D C, pp. 45–62.
Shao, Z.G., Xu, J., Ma, H.S., Zhang, L.P., 2016. Coulomb stress evolution over the past 200 years and seismic hazard along the Xianshuihe fault zone of Sichuan, China. Tectonophysics 670, 48–65.
Shen, J., Wang, Y., Song, F., 2003. Characteristics of the active Xiaojiang fault zone in Yunnan, China: a slip boundary for the southeastward escaping Sichuan-Yunnan blocks of the Tibet Plateau. J. Asian Earth Sci. 21, 1085–1096.
Shen, Z.K., Lu, J., Wang, M., Burgmann, R., 2005. Contemporary crustal deformation around the southeast borderland of the Tibetan Plateau. J. Geophys Res. 2005 (110), B11409.
Shen, Z.K., Sun, J.B., Zhang, P.Z., Wan, Y.G., Wang, M., Burgmann, R., Zeng, Y.H., Gan, W.J., Liao, H., Wang, Q.L., 2009. Slip maximum at fault junctions and rupturing of barriers during the 2008 Wenchuan earthquake groups. Nat. Geosci. 2 (10), 718–724.
Shi, F., He, H.L., Densmore, A.L., Li, A., Yang, X.P., Xu, X.W., 2016. Active tectonics of the Ganzi-Yushu fault in the southeastern Tibetan Plateau. Tectonophysics 676, 112–124.
Song, F., Wang, Y., Yu, W., Cao, Z., Shen, X., Shen, J., 1998. The Xiaojiang active fault zone. Seismological Press, Beijing, pp. 237 (in Chinese).
Wan, Y.G., Shen, Z.K., Sheng, S.Z., Xu, X., 2009. The influence of 2008 Wenchuan earthquke on surrounding faults. Acta Seismol. Sin. 31 (2), 128–139 (in Chinese with English abstract).
Wang, S.X., Jiang, F.Y., Hao, M., Zhu, L.Y., 2013. Investigation of features of present 3D crustal movement in eastern edge of Tibet plateau. Chinese J. Geophys 56 (10), 3334–3345 (in Chinese with an English abstract).
Wang, C., Huangfu, G., 2004. Crustal structure in Tengchong volcanic-geothermal area, western Yunnan, China. Tectonophysics 380, 69–87.
Wang, F., Peng, Z., Zhu, R., He, H., Yang, L., 2006. Petrogenesis and magma residence time of lavas from Tengchong volcanic field (China): evidence from U series disequilibria and 40Ar/39Ar dating. Geochem. Geophys. Geosyst. 7, 1–15.
Wang, J.J., 2010. Co-seismic, post-earthquake and inter-seismic stress triggers (Doctoral thesis). Wuhan University (in Chinese).
Wang, M., 2009. Analysis of GPS Data with High Precision and Study on Present-day Crustal deformation in China (Doctoral thesis). Institute of Geology, China Earthquake Administration (in Chinese).
Wang, Q., Qiao, X.J., Lan, Q.G., Jeffrey, F., Yang, S.M., Xu, C.J., Yang, Y.L., You, X.Z., Tan, K., Chen, G., 2011. Rupture of deep faults in the 2008 Wenchuan earthquake and uplift of the Longmen Shan. Nat. Geosci. 4, 634–640.
Wang, S., Xu, X.Y., Hu, J.F., 2015. Review on the study of crustal structure and geodynamics models for the southeast margin of the Tibetan Plateau. Chinese J. Geoophys. 58 (11), 4235–4253 (in Chinese with English abstract).
Wang, X.B., Gao, Y., Wang, Z., Yu, J.S., 2017. Research progress on deep geophysics and continental dynamic in Eastern Tibetan Plateau. Chinese J. Geophys. (in Chinses) 60 (6), 2030–2037.
Wang, Y.Z., Wang, E.N., Shen, Z.K., Wang, M., Gan, W.J., Qiao, X.J., Meng, G.J., Li, T.M., Tao, W., Yang, Y.L., Cheng, J., Li, P., 2008. GPS-constrained inversion of present-day slip rats along major faults of the Sichuan-Yunnan region. Sci. China Ser. D Earth Sci. 51 (9), 1267–1283.
Wen, X., Ma, S., Xu, X., He, Y., 2008a. Historical pattern and behavior of earthquake ruptures along the eastern boundary of the Sichuan-Yunnan faulted-block, southwestern China. Phys. Earth Planet. Int. 168, 16–36.
Wen, X.Z., 2000. Character of rupture segmentation of the Xianshuihe-Anninghe-Zemuhe fault zone, western Sichuan. Seismol. Geol. 22 (3), 239–249 (in Chinese with English abstract).
Wen, X.Z., Ma, S.L., Xu, X.W., He, Y.N., 2008b. Historical pattern and behavior of earthquake ruptures along the eastern boundary of the Sichuan-Yunnan faulted-block, southwestern China. Phys. Earth Planet. Int. 168 (1–2), 16–36.
Wen, X.Z., Xu, X.W., Zhang, R.Z., et al., 2003. Average slip-rate and recent large earthquake ruptures along the Garze-Yushu fault. Sci. China (Ser D) 46 (z2), 276–288.
Wessel, P., Smith, W.H.F., 1998. New, improved version of generic mapping tools released. EOS Trans. AGU 79, 579. http://dx.doi.org/10.1029/98EO00426.
White, L.T., Lister, G.S., 2012. The collision of India with Asia. J. Geodyn. 56–57, 7–17.
Wu, Y.Q., Jiang, Z.S., Yang, G.H., Wei, W.X., Liu, X.X., 2011. Comparison of GPS strain rate computing methods and their reliability. Geophys. J. Int. 185, 703–717.
Wu, Z.H., Zhao, G.M., Long, C.X., Zhou, C.J., Fan, T.Y., 2014. The seismic hazard assessment around south-east area of Qinghai-Xizang plateau: a preliminary results from active tectonic system analysis. Acta Geol. Sin. 88 (8), 1401–1416.
Wu, Y.Q., Jiang, Z.S., Zhao, J., Liu, X.X., Wei, W.X., Liu, Q., Li, Q., Zou, Z.Y., Zhang, L., 2015a. Crustal deformation before the 2008 Wenchuan Ms8.0 earthquake studied using GPS data. J. Geodyn. 85, 11–23.
Wu, Z.H., Long, C.Q., Fan, T.Y., Zhou, C.J., Feng, H., Yang, Z.Y., Tong, Y.B., 2015b. The arc rotational-shear active tectonic system on the southeastern margin of Tibetan Plateau and its dynamic characteristics and mechanism. Geol. Bull. China 2015;34(1):1–31.
Xie, Y., Cai, M., 1987. Compilation of historical materials of Chinese earthquake, vol.III-2. Seismological Press, Beijing, pp. 1427 (in Chinese).
Xiong, X., Shan, B., Zheng, Y., et al., 2010. Stress transfer and its implication for earthquake hazard on the Kunlun fault. Tibet. Tectonophysics 482 (1), 216–225.
Xu, R., Stamps, D.S., 2016. Present-day kinematics of the eastern Tibetan Plateau and Sichuan Basin: implications for lower crustal rheology. J. Geophys. Res. Solid Earth 121, 3846–3866.
Xu, X.M., Ding, Z.F., Shi, D.N., Li, X.F., 2013. Receiver function analysis of crustal structure beneath the eastern Tibetan plateau. J. Asian Earth Sci. 73, 121–127.
Xu, X.W., Wen, X.Z., Zheng, B.Z., Ma, W.T., Song, F.M., Yu, G.H., 2003. The latest tectonic variation pattern and dynamic sources of active blocks in Sichuan Yunnan region. 33(S1):151–162 (in Chinese).
Xu, X.W., Wen, X.Z., Zheng, R.Z., et al., 2003b. Pattern of latest tectonic motion and its dynamics for active blocks in Sichuan-Yunnan region, China. Sci. in China (Ser D) 46 (Suppl. 2), 210–226.
Xu, X.W., Wen, X.Z., Chen, G.H., et al., 2008. Discovery of the Longriba faults, eastern part of the Bayankela tectonic blockand its geodynamic implications. Sci. China Ser D 38 (5), 529–542.
Xu, X.W., Wu, X.Y., Yu, G.H., Tian, X.B., Li, K., 2017. Seismo-geological signatures for identifying M > 7.0 earthquake risk areas and their premilimary application in mainland china. Seismol. Geol. 39 (2), 219–275.
Yang, Y.Q., Liu, M., 2009. Crustal thickening and lateral extrusion during the Indo-Asian collision: a 3D viscous flow model. Tectonophysics 465, 128–135.
Yao, H.J., van der Hilst, R.D., Montagner, J.-P., 2010. Heterogeneity and anisotropy of the lithosphere of SE Tibet from surface wave array tomography. J. Geophys. Res. 115, B12307.
Yin, A., Harrison, T.M., 2000. Geologic evolution of the Himalayan-Tibetan orogen. Annu. Rev. Earth Planet. Sci. 28, 211–280.
Zhang, J., Wu, Y.Q., Liu, Q., Chen, R.H., 2013a. Relationship between plane strain rate gradient of GPS horizontal deformation and strong earthquake risk area. Acta Seismol. Sin. 35 (6), 828–835 (in Chinese with an English abstract).
Zhang, P.Z., 2008. The present tectonic deformation, strain distribution and deep dynamic process in the western Sichuan – Tibet. Plateau. 38 (9), 1041–1056 (in Chinese).
Zhang, P.Z., Gan, W.J., Shen, Z.K., 2005. A coupling model of rigid-block movement and

continuous deformation: patterns of the present-day deformation of China's continent and its vicinity. Acta Geologoca Sinica 79 (6), 748–756.
Zhang, X.M., Wang, Y., 2007. Seismic and GPS evidence for the kinematics and the state of stress of active structures in south and south-central Tibetan Plateau. J. Asian Earth Sci. 29, 283–295.
Zhang, Z.Q., McCaffrey, R., Zhang, P.Z., 2013b. Relative motion across the eastern Tibetan plateau: contributions from faulting, internal strain and rotation rates. Tectonophysics 584, 240–256.
Zhou, R., Ma, S., Cai, C., 1997a. Late Quaternary active features of the Ganzi-Yushu fault zone. Earthquake Res. China 12, 250–260 (in Chinese with English abstract).
Zhou, R.J., Wen, X.Z., Cai, C.X., et al., 1997b. Recent earthquakes and assessment of seismic tendency on the Ganzi-Yushu fault zone. Seismol. Geol. 19 (2), 115–124 (In Chinese).
Zhu, J.S., Wang, X.B., Yang, Y.H., Fan, J., Cheng, X.Q., 2017. The crustal flow beneath the eastern margin of the Tibetan Plateau and its process of dynamic. Chinese J. Geophys. (in Chinese) 60 (6), 2038–2057.
Zhu, Z.M., Hayao, M., Gui, R.J., Xu, S.Q., Liu, Y.Y., 2006. Palemagnetic constraints on the extent of the stable body of the South China Block since the Cretaceous: new data from the Yuanma Basin, China. Earth Planet. Sci. Lett. 248, 533–544.
Zou, Z.Y., Jiang, Z.S., Wu, Y.Q., Wei, W.X., Fang, Y., Liu, X.X., 2015. Dynamic characteristics of crustal movement in north-south seismic belt from GPS velocity field before and after the Wenchuan Earthquake. Chinese J. Geoophys. 58 (5), 1597–1609 (in Chinese with English abstract).
Zhou, R.J., Li, Y., Densmore, A.L., et al., 2006. Active tectonics of the eastern margin of the Tibetan Plateau. J. Mineral. Petrol. (in Chinese) 26 (2), 40–51.